Paleobiology, 44(3), 2018, pp. 530–545
DOI: 10.1017/pab.2018.14

PALEOBIOLOGY
A PUBLICATION OF THE Paleontological SOCIETY

Ecophenotypy, temporal and spatial fidelity, functional morphology, and physiological trade-offs among intertidal bivalves

John Warren Huntley, James D. Schiffbauer, Teresa D. Avila, and Jesse S. Broce

Abstract.—Ecophenotypic variation in populations is driven by differences in environmental variables. In marine environments, ecophenotypic variation may be caused by differences in hydrodynamic conditions, substrate type, water depth, temperature, salinity, oxygen concentration, and habitat heterogeneity, among others. Instances of ecophenotypic variation in modern and fossil settings are common, but little is known about the influences of time averaging and spatial averaging on their preservation. Here we examine the shell morphology of two adjacent populations, both live collected and death assemblages, of the infaunal, suspension-feeding, intertidal bivalve *Leukoma staminea* from the well-studied Argyle Creek and Argyle Lagoon locations on San Juan Island, Washington. Individuals in the low-energy lagoon are free to burrow in the fine-grained substrate, while clams in the high-energy creek are precluded from burrowing in the rocky channel. Our results demonstrate variation in size and shape between the adjacent habitats. Lagoon clams are larger, more disk-shaped, and have relatively larger siphons than their creek counterparts, which are smaller, more spherical in shape, and have a relatively shallower pallial sinus. This ecophenotypy is preserved among death assemblages, although with generally greater variation due to time averaging and shell transport. Our interpretation is that ecophenotypic variation, in this case, is induced by differing hydrodynamic regimes and substrate types, cumulatively resulting in physiological trade-offs diverting resources from feeding and respiration to stability and shell strength, all of which have the potential to be preserved in the fossil record.

John Warren Huntley, Teresa D. Avila, and Jesse S. Broce. Department of Geological Sciences, University of Missouri, 101 Geology Building, Columbia, Missouri 65211, U.S.A. E-mail: huntleyj@missouri.edu.*
*Present address: School of Earth Sciences, Ohio State University, Columbus, Ohio 43210, U.S.A.

James D. Schiffbauer. Department of Geological Sciences and X-Ray Microanalysis Core Facility, University of Missouri, 101 Geology Building, Columbia, Missouri 65211, U.S.A.

Accepted: 21 March 2018
Published online: 30 May 2018
Data available from the Dryad Digital Repository: https://doi.org/10.5061/dryad.2bs5231

Introduction

A sound understanding of the magnitude and sources of variation of both the size and shape of extinct organisms is fundamental for accurate interpretation of data in paleobiological inquiry. Such variation may be attributed to a variety of sources, including ontogenetic, ecological, evolutionary, or taphonomic processes. Ecophenotypic variation is intraspecific variation in size or shape driven by differences in environmental variables acting on genetically similar populations. Environmentally driven differences in size and shape have been identified in a broad range of taxa throughout the history of metazoans and have been attributed to a variety of drivers, including hydrodynamic conditions, substrate type, water depth, immersion time in intertidal environments, temperature, salinity, oxygen concentration, pH, habitat/bathymetric heterogeneity, population density, and food availability (e.g., Bottjer 1980; Kemp and Bertness 1984; Daley 1999; Wilk and Bieler 2009; Zieritz and Aldridge 2009; Clewing et al. 2015; Piovesan et al. 2015; Schlüter 2016; Penny et al. 2017). Correctly recognizing ecophenotypic variation can help one avoid mistakes in taxonomic identification and can assist in the interpretation of paleoenvironments based upon their influence on such taxa.

Though little has been published on the influence of taphonomic processes on the preservation of ecophenotypic variation specifically, such research has addressed the preservation of morphological variation in general. Time averaging, the temporal mixing of multiple generations of organisms within a stratigraphic interval, is generally thought to result in the preservation of greater morphological variability within a deposit than had existed in single populations (Wilson 1988; Bush et al. 2002),

 0094-8373/18

though the extent depends upon the tempo and mode of evolution as well as the extent of time averaging (Kidwell and Holland 2002; Hunt 2004a, 2004b). Presumably, time averaging of ecophenotypic variation would result in a similar "smearing" of morphological variability as the driving environmental variables change through time. Spatial mixing of fossils by out-of-habitat transport is rare, except in predictable depositional settings (e.g., rivers, turbidites) and taxa (e.g., bloated vertebrate carcasses, chambered-shell cephalopods), though within-habitat transport is likely common (Kidwell and Holland 2002). Within-habitat postmortem transport of skeletal material would also likely reduce the spatial fidelity of ecophenotypic variation in the fossil record, though again, these ideas have yet to be evaluated.

Leukoma staminea, previously referred to as *Protothaca staminea* by Huntley (2007; see Coan and Valentich-Scott 2012), is an infaunal, suspension-feeding bivalve from the Veneridae family that is common in gravelly, sandy, and muddy substrates in protected bays along northern Pacific coasts (Kozloff 2000; Huber 2010) and is particularly common in the vicinity of North Bay, San Juan Island, WA (Fig. 1). Argyle Lagoon is a low-energy, tidally influenced body of marine water whose mud/sand substrate remains submerged in the interior, with only its margins exposed during low tides. The lagoon maintains connection and circulation with the open waters of Argyle and North Bays via Argyle Creek, a shallow, high-energy tidal creek with a gravel/sand substrate whose thalweg is also not completely exposed during low tide. These differences in substrate impose differing life modes upon *L. staminea* individuals, with a typical infaunal life mode in Argyle Lagoon and an atypical epifaunal life mode in Argyle Creek. Live-collected bivalves from the creek have been shown to be significantly smaller and infested more frequently by shell-altering digenean trematode parasites (indicated by the presence of oval-shaped pits with raised rims on the interior of the host) than lagoon bivalves (Huntley 2007). Likewise, epifaunal specimens suffer higher taphonomic alteration than their infaunal counterparts (Lazo 2004). Lazo (2004) asserted that the differences in life

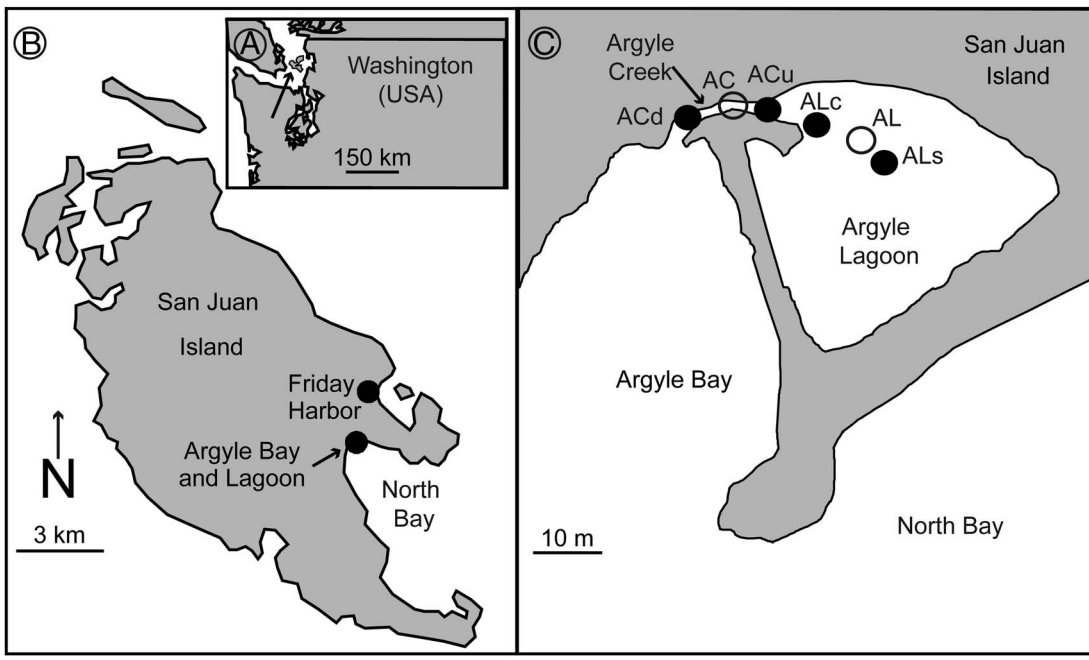

FIGURE 1. Location map of study: A, Washington; B, San Juan Island; and C, Argyle Creek and Argyle Lagoon. Live-collected specimen locations are indicated by open circles (AC, Argyle Creek; AL, Argyle Lagoon). Death-assemblage locations are indicated by solid circles (ACd, Argyle Creek downstream; ACu, Argyle Creek upstream; ALc, Argyle Lagoon spit-side channel; ALs, Argyle Lagoon surface). Figure modified from Huntley (2007).

mode were not reflected in shell morphology, but a visual inspection of the specimens of Huntley (2007) suggests otherwise. The purposes of this study are: (1) to test for variation in size and shape of live-collected conspecific intertidal bivalves living within close proximity on differing substrates with differing life modes, (2) to test for linkages between trematode parasitism and bivalve morphology, (3) to test the fidelity of these signals within adjacent death assemblages, and (4) to examine the ecological underpinnings and implications of such variation, if present.

Materials and Methods

Live specimens of *L. staminea* were collected in both the creek (AC; epifaunal individuals; the gravel substrate precludes burrowing) and the lagoon (AL; infaunal individuals; mud, silt, to very fine sand) in August 2004 (Huntley 2007). Surficial death assemblages were collected in August 2006 from four locations: downstream from the AC location (ACd); upstream from the AC location (ACu); in the higher-energy, spit-side channel at the juncture of the lagoon and creek (ALc; coarse sand, gravel, shell bed substrate); and from the lower-energy surface of the lagoon adjacent to the location of the live-collected sample (ALs; Fig. 1).

Live specimens were sacrificed and cleaned with a scalpel and small brush. Valves from death assemblages were soaked in 10% H_2O_2 solution to remove desiccated algae and cleaned physically with a small brush. Valves from death assemblages were examined for matches. The pallial line, pallial sinus, and adductor muscle attachment scars of these valves were outlined in pencil so as to accentuate their visibility. Photographs of the interior of these valves were made with a Nikon D600 digital SLR camera on a Kaiser eVision copy-stand for a standardized orientation. Specimens and scale bars were placed near the center of view, and consistent camera settings were maintained for images of all specimens (Collins and Gazley 2017). The left valves of the live-collected specimens, the right paired valves from the death assemblages, and the left and right singletons from the death assemblages were used for further analysis. Mirrored images of the left valves were used such that all data were extracted from a right-valve orientation.

Ten true landmarks (Fig. 2A, 1–10) and four pseudolandmarks (Fig. 2A, 11–14) were selected to quantify the morphology of *L. staminea* valves from scaled images in ImageJ freeware. The x- and y-coordinates of the landmarks were collected from the same specimen (ACPS01) 90 times to assess operator error. The error about each of the landmarks, with the exception of landmark 2, was distributed in a circular pattern (Fig. 2B), suggesting that error was random and did not display a preferred orientation. Landmark 2 and pseudolandmarks 11–14 displayed a linear

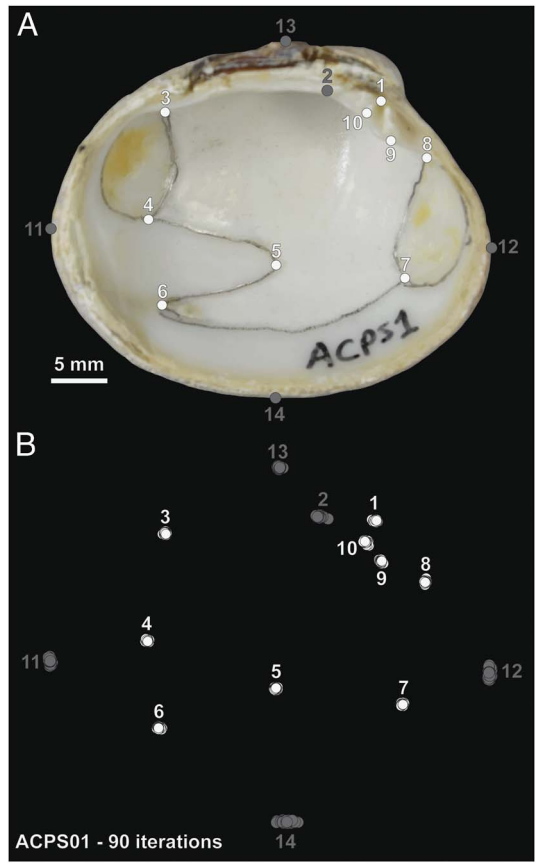

FIGURE 2. *Leukoma staminea* and landmarks. A, *Leukoma staminea* live collected in Argyle Creek (ACPS01) with landmarks indicated by circles. B, Procrustes-transformed x- and y-coordinates of all landmarks measured on the same individual 90 times to assess operator error. Landmark 2 and pseudolandmarks 11–14, shown in gray, displayed linear variation and were not used in further analyses. Landmarks in white (1, 3–10) displayed circular variation about the mean and were further analyzed.

orientation of error tangential to the shell margin (Fig. 2B) and were not included in further analyses.

Centroid size, a proxy for body size (the square root of the sum of squared distances of the landmarks from the centroid), was calculated for each valve from landmarks 1 and 3–10. The landmark coordinate data were then subjected to a generalized least-squares Procrustes transformation to eliminate differences attributable to orientation, position, and size. A principal components analysis (PCA) was conducted on the Procrustes-transformed landmark data on the variance–covariance matrix. To aid interpretation of this morphospace, thin-plate spline analyses were used to produce deformed grids and expansion factors for four select specimens, from opposing extremes of the morphospace, relative to the mean configuration of the Procrustes-transformed coordinates. Further, point cloud data of the interior of these select bivalves were collected using a FARO Arm laser scanner (35 μm resolution). Three-dimensional models were produced in InnovMetric PolyWorks software. These models were compared in InnovMetric IMinspect software by scaling opposing shells to the same centroid size, conducting a best-fit alignment of the valves' interior surfaces using the *alignment* tool, and producing a color map illustrating topographic differences using the *measure deviation* tool. The 2D surface areas of the anterior and poster adductor muscle scars were measured from the photographs using ImageJ freeware (Schneider et al. 2012). The length of the pallial sinus was calculated from the landmark data as the distance between landmark 5 and the midpoint of a straight line connecting landmarks 4 and 6. Allometric coefficients were calculated for the muscle scars and the pallial sinus for the live-collected specimens by environment (AC and AL). The allometric coefficient is calculated as the slope of the reduced major axis regression model between the natural log-transformed sizes of the anatomical feature (surface area for muscle scars, length for pallial sinus) with the natural log-transformed centroid size. Randomizations (10,000 iterations) were conducted in SAS (version 9.4) to determine the 95% and 99% confidence intervals for the range of variance values expected by random chance (similar to an ANOVA) for centroid size, PC 1 values, and PC 2 values from each sample. Calculation of centroid size and Procrustes transformation were performed in PAST freeware (version 2.17c) (Hammer et al. 2001). Reduced major axis regressions, PCA, and the calculation and plotting of density values for centroid size and PC variables were performed in R freeware using the following packages: 'ggplot2,' 'plyr,' 'dplyr,' 'factoextra,' 'lmodel2,' 'ggpubr,' and 'ggridges' (Wickham 2009, 2011; Legendre 2014; Kassambara 2017; Kassambara and Mundt 2017; R Core Team 2017; Wickham et al. 2017; Wilke 2017). An alpha of 0.05 is assumed for all statistical tests unless otherwise stated.

Results

Body size varied significantly among the live-collected and death-assemblage samples (Fig. 3, Table 1). Live-collected specimens from Argyle Creek were significantly smaller than their counterparts in all other samples, whether live collected or death assemblage (Table 1). There was no significant difference in body size between the two death assemblages from Argyle Creek. Live-collected valves from AL were significantly larger than valves in the ALc death assemblage and significantly smaller than valves in the ALs death assemblage. The median body size of the ALs death assemblage was significantly greater than the median body size of all other samples, living or dead (Table 1). Variance of body size was greater in the creek death assemblages (ACd, ACu) and the spit-side channel death assemblage of the lagoon (ALc) than in the live-collected assemblages of both the creek (AC) and lagoon (AL) or the surface death assemblage of the lagoon (ALs; Table 1). Indeed, body-size variance values of AC, AL, and ALs fall below the 99% confidence interval calculated from the randomization (Table 2).

The PCA results show distinct positions of the samples in the landmark-derived morphospace (Fig. 4). The first two principal components (PC 1 and PC 2) account for 45.5% of the size-free morphological variation (28.3% and 17.2%, respectively) and illustrate the most

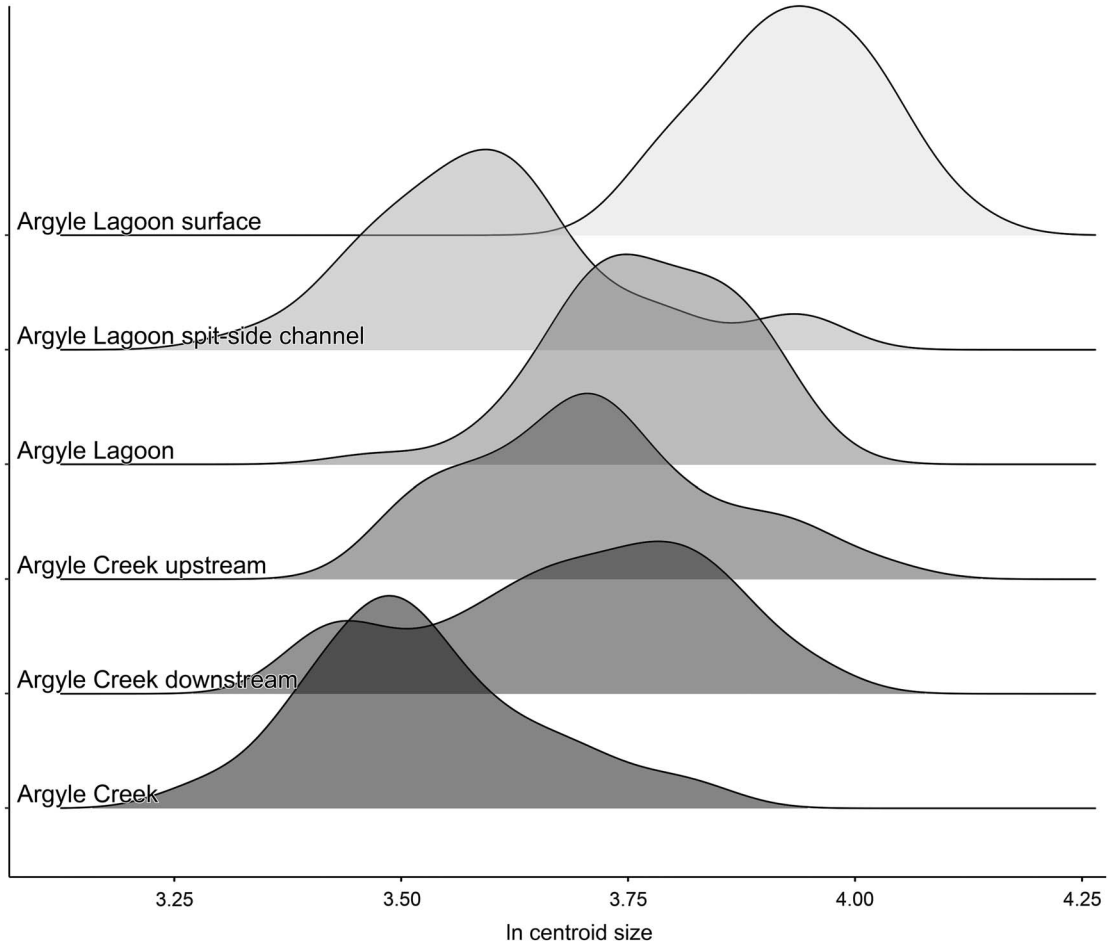

FIGURE 3. Natural log-transformed, centroid size-density distributions for live-collected (AC and AL) and death-assemblage (ACd, ACu, ALc, and ALs) specimens of *Leukoma staminea* from Argyle Creek and Argyle Lagoon.

TABLE 1. Body-size (centroid-size) summary statistics and *p*-values of pairwise Wilcoxon tests for median centroid-size values of *Leukoma staminea* from Argyle Creek (AC) and Argyle Lagoon (AL). ACd, downstream from the AC location; ACu, upstream from the AC location; ALc, in the higher-energy, spit-side channel at the juncture of the lagoon and creek; ALs, from the lower-energy surface of the lagoon adjacent to the location of the live-collected sample. ns, not significant, $>\alpha_{Bonferroni}$ (0.05/15 = 0.003).

	AC	AL	ACd	ACu	ALc	ALs
n	46	47	22	37	53	24
Minimum	26.6	32.2	29.9	32.5	27.7	43.8
Maximum	46.4	52.3	52.1	56.2	51.7	61.0
Median	33.2	43.4	40.7	40.3	36.3	50.7
Variance	20.1	18.2	38.3	33.6	30.6	20.8
Wilcoxon *p*-values						
AC	–	–	–	–	–	–
AL	1.88E-15	–	–	–	–	–
ACd	5.84E-05	ns	–	–	–	–
ACu	1.04E-08	ns	ns	–	–	–
ALc	2.65E-03	4.53E-09	ns	4.63E-04	–	–
ALs	2.20E-16	8.00E-09	2.99E-08	9.49E-09	2.14E-10	–

distinction between the samples (Supplemental Figs. 1 and 2). The surface death-assemblage and live-collected specimens from Argyle Lagoon display more positive PC 1 values, while live-collected Argyle Creek specimens display more negative values. The upstream

TABLE 2. Results of 10,000-iteration randomizations for body-size variance values. Percentile values were used to calculate 95% and 99% confidence intervals for variance. Variance values that fall outside of one or both confidence intervals are in bold. AC, Argyle Creek; ACd, downstream from the AC location; ACu, upstream from the AC location; AL, Argyle Lagoon; ALc, in the higher-energy, spit-side channel at the juncture of the lagoon and creek; ALs, from the lower-energy surface of the lagoon adjacent to the location of the live-collected sample.

Body size	AC	AL	ACd	ACu	ALc	ALs
Variance	**20.1**	**18.2**	38.3	33.6	**30.6**	**20.8**
0.5th percentile	29.0	28.8	21.4	27.4	30.3	22.0
2.5th percentile	33.8	33.6	26.7	31.9	34.5	27.7
97.5th percentile	69.1	69.5	78.3	71.7	68.1	77.5
99.5th percentile	75.7	76.4	88.5	79.6	73.1	86.7

and downstream creek death-assemblage specimens overlap nearly completely and display more central PC 1 values (Fig. 4, Table 3). Specimens from the Argyle Lagoon spit-side channel death assemblage display a broad range of PC 1 values, again centered near a value of zero. The median PC 1 value for AC live-collected specimens is significantly more negative than the median PC 1 scores for all other samples, either live collected or death assemblage (Table 3). The median PC 1 value for the ALs sample is significantly more positive than all other samples except for AL (Table 3). Variation of PC 1 scores, quantified as variance, is significantly lower than expected by random chance for the AL live-collected sample (<<99% CI) and the ALs death assemblage (<95% CI). The PC 1 variance values of the remaining samples fell within the envelope of values expected by random chance (Table 4). There is no significant difference between the median PC 1 values of parasitized and nonparasitized valves in the AL ($p = 0.405$) and AC ($p = 0.921$) samples (Fig. 4).

Similar to PC 1, Bonferroni-corrected Wilcoxon tests reveal significant differences in median PC 2 score values between samples (Table 5). The median PC 2 score for the AL sample was significantly higher than the median PC 2 scores of the AC, ACu, and ALc samples. There is no statistically significant difference in median PC 2 scores for AL and ALs (Table 5). The median PC 2 value of the AC sample is statistically indistinguishable from ACd, ACu, and the ALs samples. The ALc median PC 2 value is significantly lower than all samples except ACu. The variance of the AC PC 2 value is slightly less than the lower 95% confidence interval. The PC 2 variance values for all other samples falls within the envelope of that which is expected by random chance based upon the randomization results (Table 6). The median PC 2 value of parasitized AL individuals is significantly higher than nonparasitized AL individuals ($p = 0.007$). Conversely, the median PC 2 value of parasitized AC individuals is significantly lower than nonparasitized AC valves ($p = 0.031$).

Thin-plate spline analyses relative to the mean Procrustes-transformed landmark data configuration were conducted on four specimens that represented distal values on one of the axes in the PC 1 versus PC 2 space and a value near zero on the other axis in order to aid in the interpretation of the morphospace (Fig. 5). Expansion factors were calculated in each cell of the 20 line by 20 line grid (19 cells by 19 cells) and are displayed in cool and warm colors indicating contraction and expansion, respectively. Positive PC 1 values correspond with a deep pallial sinus, while negative PC 1 values correspond to a shallow pallial sinus. The deepened pallial sinus is the result of posterior expansion and anterior contraction, while the shallower pallial sinus is due to the opposite pattern: anterior expansion and posterior contraction (Fig. 5). The strong visual difference in expansion and contraction of the anterior and posterior portions of the shell along PC 1 could also indicate diverging size patterns of the adductor muscles. Morphological variation along the PC 2 axis is more subdued and is related to dorsal expansion, with negative PC 2 values and ventral expansion corresponding to positive PC 2 values. The comparison of 3D models demonstrates that positive PC 1 values are associated

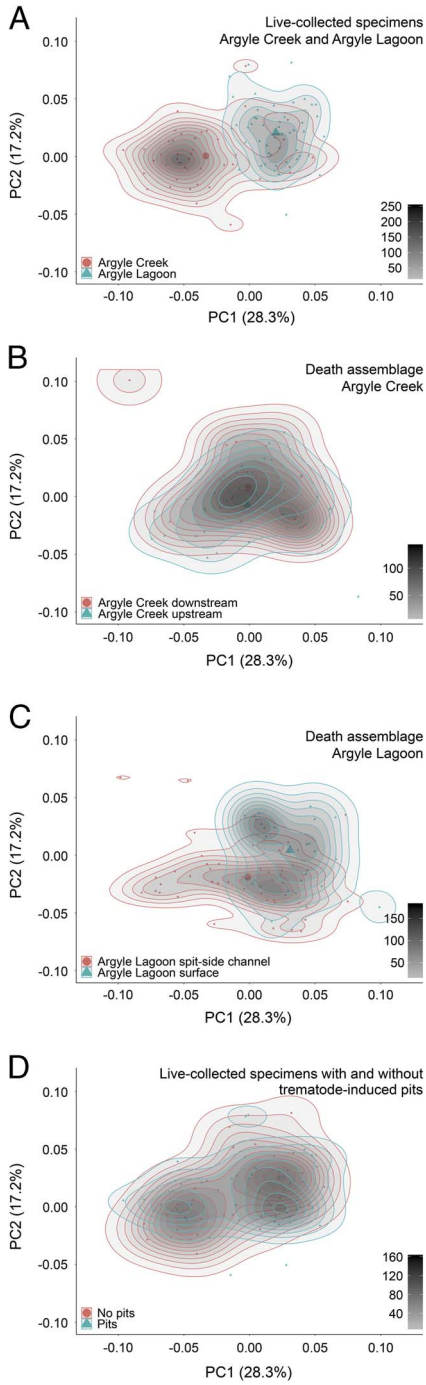

FIGURE 4. Principal components analysis of Procrustes-transformed landmark data of *Leukoma staminea* from Argyle Creek and Argyle Lagoon (PC 1 v. PC 2). A, Comparison of Argyle Creek and Argyle Lagoon live-collected samples. B, Comparison of Argyle Creek death assemblages. C, Comparison of Argyle Lagoon death assemblages. D, Comparison of parasitized and nonparasitized live-collected samples from Argyle Creek and Argyle Lagoon. See Supplemental Fig. 1 for scree and loadings plots.

with flatter shells with an elevated central interior surface and depressed commissural margin, whereas negative PC 1 values are associated with deeper valves with a depressed central interior surface and elevated commissural margin. Morphological differences along the PC 2 axis are less clear than those in PC 1, but generally illustrate depressed ventral margins with positive PC 2 values and possibly elevated ventral margins with negative PC 2 values.

The allometric coefficients of both anterior and posterior adductor muscle scars are statistically indistinguishable between live-collected specimens from AC and AL (Fig. 6). Similarly, the ratios between natural log-transformed muscle scar area and natural log-transformed centroid size are also indistinguishable between the creek and lagoon (Mann-Whitney U, $p_{\text{anterior}} = 0.72$ and $p_{\text{posterior}} = 0.33$). The allometric coefficient of the pallial sinus in creek live specimens is significantly larger than that of lagoon counterparts (Fig. 6). The ratio between the natural log-transformed pallial sinus length and natural log-transformed centroid size is significantly smaller for creek specimens than for those from the lagoon (Mann-Whitney U, $p = 7.37 \times 10^{-11}$; Fig. 6).

Discussion

Spatial Variation of Body Size and Live–Dead Fidelity.—Live-collected specimens from the creek were significantly smaller than their live-collected counterparts from the lagoon (Fig. 3). Huntley (2007) first reported this pattern and speculated that it could be due to a number of non–mutually exclusive factors:

1. stress in creek clams due to the inability to burrow in the gravel substrate and occasional subaerial exposure;
2. higher trematode prevalence in creek clams relative to lagoon clams;
3. increased susceptibility to durophagous predators like crabs, birds, and raccoons as the combined result of forced epifaunality and higher boring spionid prevalence (thereby weakening shells) among creek clams relative to lagoon clams;

TABLE 3. Principal component 1 (PC 1) score summary statistics and *p*-values of pairwise Wilcoxon tests for median PC 1 values for each sample of *Leukoma staminea* from Argyle Creek (AC) and Argyle Lagoon (AL). ACd, downstream from the AC location; ACu, upstream from the AC location; ALc, in the higher-energy, spit-side channel at the juncture of the lagoon and creek; ALs, from the lower-energy surface of the lagoon adjacent to the location of the live-collected sample. ns, not significant, $>\alpha_{Bonferroni}$ (0.05/15 = 0.003).

	AC	AL	ACd	ACu	ALc	ALs
n	46	47	22	37	53	24
Minimum	−0.096	−0.015	−0.091	−0.074	−0.098	−0.023
Maximum	0.048	0.057	0.042	0.083	0.075	0.099
Median	−0.044	0.020	−4.61E-04	−0.005	0.009	0.027
Variance	1.28E-03	3.59E-04	1.30E-03	1.33E-03	1.68E-03	6.75E-04
Wilcoxon *p*-values						
AC	–	–	–	–	–	–
AL	1.98E-11	–	–	–	–	–
ACd	9.58E-04	ns	–	–	–	–
ACu	6.99E-05	0.001	ns	–	–	–
ALc	1.77E-04	ns	ns	ns	–	–
ALs	9.64E-10	ns	0.002	1.75E-04	0.002	–

TABLE 4. Results of 10,000-iteration randomizations for principal component 1 (PC 1) variance values. Percentile values were used to calculate 95% and 99% confidence intervals for variance. Variance values that fall outside of one or both confidence intervals are in bold. AC, Argyle Creek; ACd, downstream from the AC location; ACu, upstream from the AC location; AL, Argyle Lagoon; ALc, in the higher-energy, spit-side channel at the juncture of the lagoon and creek; ALs, from the lower-energy surface of the lagoon adjacent to the location of the live-collected sample.

PC 1	AC	AL	ACd	ACu	ALc	ALs
Variance	0.0013	**0.0004**	0.0013	0.0013	0.0017	**0.0007**
0.5^{th} percentile	0.0008	0.0009	0.0006	0.0008	0.0009	0.0006
2.5^{th} percentile	0.0010	0.0010	0.0008	0.0010	0.0010	0.0008
97.5^{th} percentile	0.0021	0.0021	0.0024	0.0021	0.0021	0.0023
99.5^{th} percentile	0.0023	0.0022	0.0027	0.0024	0.0022	0.0026

TABLE 5. Principal component 2 (PC 2) score summary statistics and *p*-values of pairwise Wilcoxon tests for median PC 2 values for each sample of *Leukoma staminea* from Argyle Creek (AC) and Argyle Lagoon (AL). ACd, downstream from the AC location; ACu, upstream from the AC location; ALc, in the higher-energy, spit-side channel at the juncture of the lagoon and creek; ALs, from the lower-energy surface of the lagoon adjacent to the location of the live-collected sample. ns, not significant, $>\alpha_{Bonferroni}$ (0.05/15 = 0.003).

	AC	AL	ACd	ACu	ALc	ALs
n	46	47	22	37	53	24
Minimum	−0.059	−0.050	−0.026	−0.087	−0.066	−0.057
Maximum	0.078	0.081	0.101	0.046	0.068	0.043
Median	−0.001	0.0217	−0.002	−0.004	−0.023	0.010
Variance	5.57E-04	6.90E-04	1.09E-03	7.80E-04	7.66E-04	8.01E-04
Wilcoxon *p*-values						
AC	–	–	–	–	–	–
AL	8.31E-05	–	–	–	–	–
ACd	ns	ns	–	–	–	–
ACu	ns	1.51E-05	ns	–	–	–
ALc	1.26E-05	1.76E-10	4.92E-04	ns	–	–
ALs	ns	ns	ns	ns	9.88E-04	–

4. variation influenced by differing hydrodynamic regimes in the creek and lagoon; and
5. the samples representing two distinct cohorts.

It is difficult to test among these options without specific knowledge of the ontogenetic age of individuals and differences in predation intensity by durophagous predators between the creek and lagoon environments. Growth increments are not reliable indicators of ontogenetic age in *L. staminea* (Berta 1976; Hughes and Clausen 1980), and calculating age estimates via stable isotope geochemistry is beyond the scope of this project. Further, these are either live-collected or whole dead-collected valves

TABLE 6. Results of 10,000-iteration randomizations for principal component 2 (PC 2) variance values. Percentile values were used to calculate 95% and 99% confidence intervals for variance. Variance values that fall outside of one or both confidence intervals are in bold. AC, Argyle Creek; ACd, downstream from the AC location; ACu, upstream from the AC location; AL, Argyle Lagoon; ALc, in the higher-energy, spit-side channel at the juncture of the lagoon and creek; ALs, from the lower-energy surface of the lagoon adjacent to the location of the live-collected sample.

PC 2	AC	AL	ACd	ACu	ALc	ALs
Variance	**0.0006**	0.0007	0.0011	0.0008	0.0008	0.0008
0.5^{th} percentile	0.0005	0.0005	0.0003	0.0004	0.0005	0.0004
2.5^{th} percentile	0.0006	0.0006	0.0004	0.0005	0.0006	0.0005
97.5^{th} percentile	0.0014	0.0013	0.0016	0.0014	0.0013	0.0016
99.5^{th} percentile	0.0015	0.0015	0.0018	0.0016	0.0015	0.0018

and would not provide a reliable record of durophagous predation intensity. Acquiring such data would necessitate extensive field observations, because most durophagous predators in question (i.e., birds and raccoons) remove prey items from this environment.

In general, the habitat-based discrepancy in *L. staminea* body size identified in the live-collected samples is preserved in the death assemblages. Both creek death assemblages, indistinguishable from one another, are significantly smaller than the lagoon surface death assemblage; however, they are larger than the spit-side channel death assemblage from the lagoon. This discrepancy is likely attributable to the preferential transport of smaller creek clams into the lagoon during flood tide as indicated by the general morphology of shell accumulations where the channel enters the lagoon (similar to a flood-tide delta). Notably, the median sizes of creek death-assemblage bivalves are significantly larger than live-collected creek clams. Similarly, the ALs death assemblage is, on average, significantly larger than the live clams from the lagoon. These results suggest that death assemblages accumulate a greater range of body-size variation than seen in the ecological snapshot of live-collected specimens—presumably a signal of time averaging superimposed onto that of environmentally influenced size distinctions.

Spatial Variation of Morphology and Live–Dead Fidelity.—The size-free morphological analysis via PCA of Procrustes-transformed 2D landmark data indicates significant differences in bivalve morphology between samples. This discrepancy is most apparent when comparing the central tendency and distribution of live-collected specimens. Live specimens from the lagoon have significantly more positive PC 1 values than corresponding live-collected creek specimens (Fig. 4). Moreover, the variation of PC 1 values for live lagoon specimens is less than that of the creek specimens. This variance of lagoon specimens is much less (<<99% CI) than expected by random chance (Table 4). The morphological variability of AC clams is elevated, by comparison, and falls within the confidence intervals calculated by the randomization. These findings suggest that live creek and lagoon clams were either not drawn from a single population or they were sorted during life. Contrary to the findings of Lazo (2004), there are strong morphological differences between *L. staminea* individuals living in the lagoon versus those that live in the creek. It seems that morphological variation is quite low when the clams are allowed to occupy their preferred infaunal life mode in the lagoon, but there is a significant shift in median morphology and an increase in morphological variance when the clams are restricted to epifaunal life modes in the gravel substrate of the creek. These results provide strong evidence for morphological differences in bivalves occupying spatially proximal habitats of strongly diverging substrate types and hydrodynamic regimes (Huntley 2007).

Similar to the results for body size, and also contrary to the suggestion of Lazo (2004), the spatial distribution of diverging morphologies is broadly preserved within the death assemblages. Median PC 1 scores decrease in value from the lagoon surface to the creek death assemblages, though the differences among the downstream creek, upstream creek, and

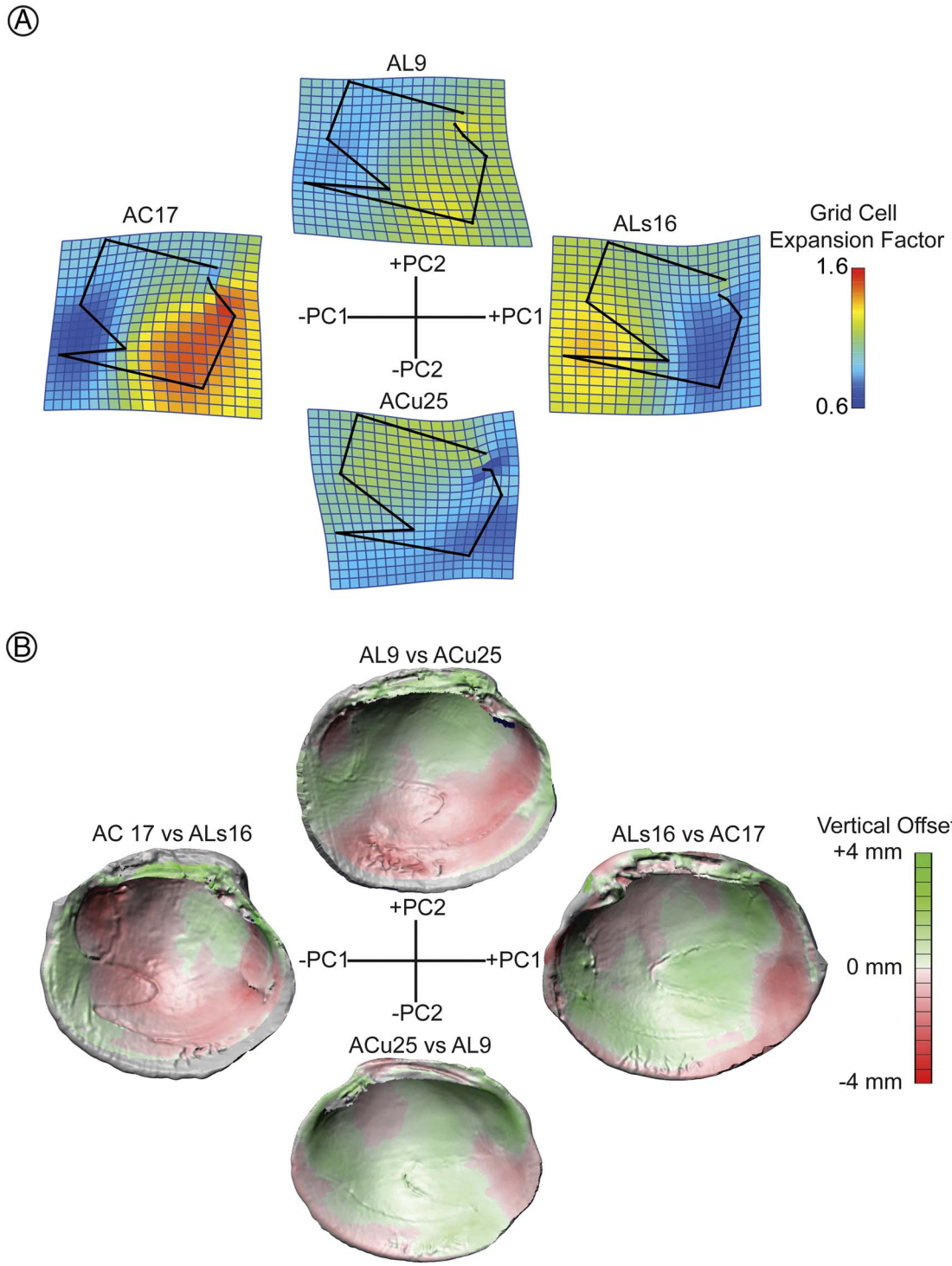

FIGURE 5. Comparison of morphological exemplars. A, Thin-plate spline analyses of select valves compared with the mean landmark morphology. Color grid indicates expansion factor of area within each grid cell (expansion in warm colors and constriction in cool colors). Landmarks are indicated by black dots and are connected by black lines. B, Vertical surface deviation between PC 1 exemplars and PC 2 exemplars. Green indicates positive offset; red indicates negative offset.

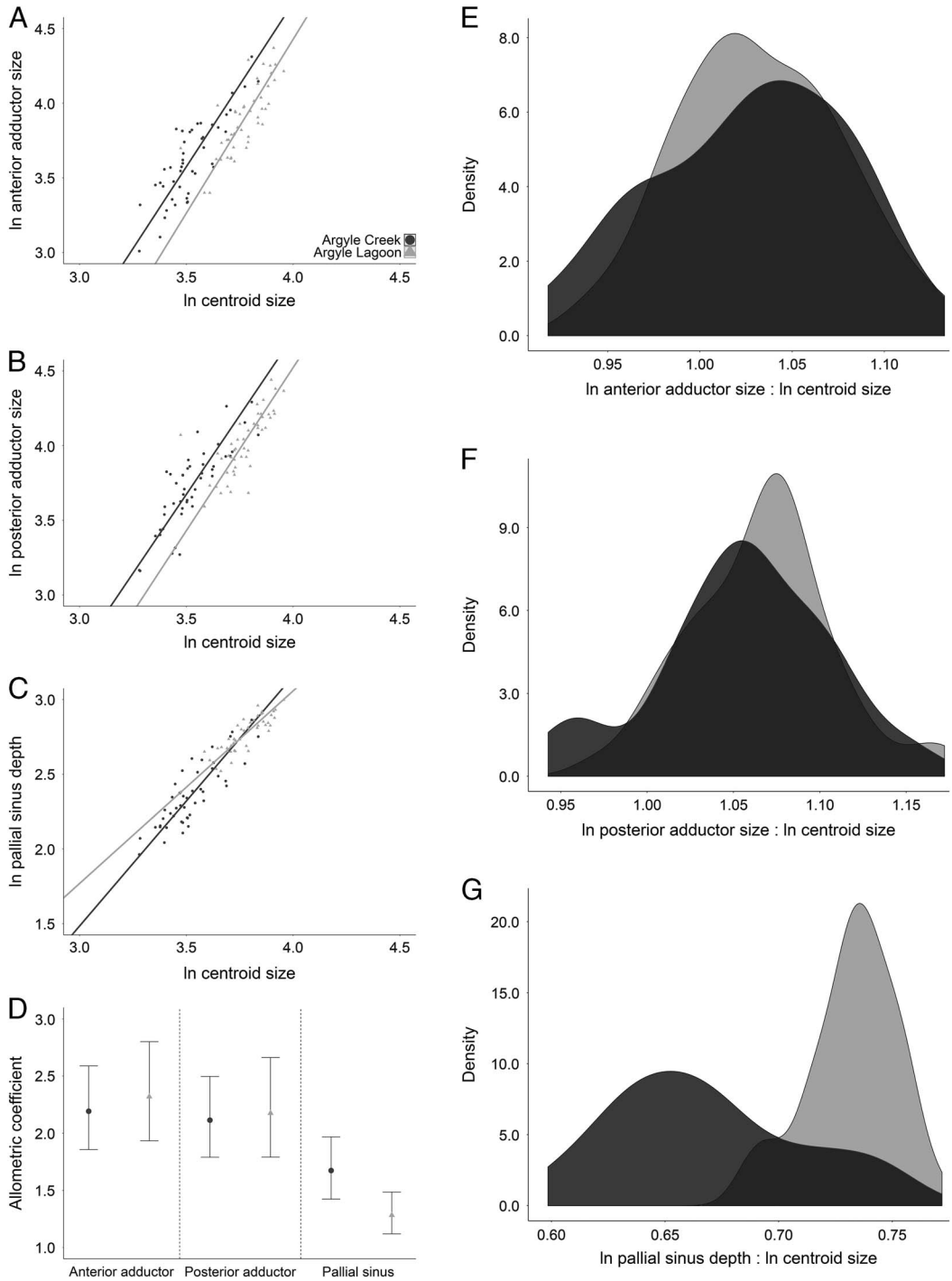

FIGURE 6. Morphological analysis of adductor muscle scar area and pallial sinus length of live-collected valves from AC and AL. A, Biplot and reduced major axis (RMA) regression model of anterior adductor muscle scar area and centroid size. B, Biplot and RMA of posterior adductor muscle scar area and centroid size. C, Biplot and RMA of pallial sinus length and centroid size. D, Allometric coefficients and bootstrapped 95% confidence intervals of adductor muscle scars and pallial sinus. E, Density distributions of natural log anterior adductor area:natural log centroid size. F, Density distributions of natural log posterior adductor area:natural log centroid size. G, Density distributions of natural log sinus length:natural log centroid-size ratios. Argyle Creek in dark gray; Argyle Lagoon in light gray.

lagoon spit-side channel samples are statistically indistinguishable.

The Accumulation of Variance in Death Assemblages and Implications for the Fossil Record.—The variation of both body size and morphology was generally greater in death assemblages than in living organisms. The variance values of body size for both live-collected samples fell below the randomization-derived 99% confidence intervals, while all death assemblages, except ALs, fell within the confidence intervals, indicating substantially lower variation among the living. This result is expected, because death assemblages are likely time averaged, comprising individuals from many generations. This pattern could have been further promoted by a seasonal bias in sample collection, typically in summer. Perhaps the live-collected clams would have been larger on average if collected later in the season.

Elevated body-size variation among creek death assemblages could indicate spatial mixing of bivalves from the creek and lagoon. Alternatively, increased variation could be the result of more extensive time averaging in Argyle Creek than in Argyle Lagoon. Lazo (2004) demonstrated higher taphonomic scores (poor preservation) for both live and dead clams from Argyle Creek relative to those from the lagoon, suggesting that fossilization potential, and thus time averaging, was greater for lagoon clams and less for creek clams. This serves as an argument against increased time averaging in the creek resulting in greater size variability. Body-size variation values in the spit-side channel and lagoon surface death assemblages were less than the 95% and 99% confidence intervals, respectively. The lagoon surface sample location has a fine-grained substrate, suggesting low hydrodynamic energy and little spatial averaging due to physical processes. The geomorphology of the spit-side channel, however, suggests an influx of material from the creek into the margin of the lagoon contrary to the low variation in body-size values.

The elevated PC 1 variance values for the creek and spit-side channel death assemblages, which fall within the 95% confidence intervals, could also be the result of increased time averaging in the higher-energy environments, but again this seems unlikely, as Lazo (2004) reported significantly poorer preservation among creek clams. Instead, the increased morphological variance values among these three death assemblages likely result from spatial mixing due to shell transport in these higher-energy environments. Such an interpretation is consistent with a considerably lower variance value (< lower 95% CI) of the lagoon surface death assemblage sourced from a low-energy setting that likely experienced very little shell transport. The similarly muted morphological variance values for the living lagoon clams and the lagoon surface death assemblage are consistent with the results of Krause (2004) that demonstrated statistically nonsignificant differences in brachiopod morphology between live-collected and death-assemblage specimens in deeper-water settings in the nearby San Juan Channel. Despite the significant difference in median PC 1 scores of live creek and live lagoon clams, there is substantial overlap of creek clams in the morphospace occupied by lagoon clams, suggesting that some individuals developed the typical morphology living in the lagoon and were then transported in vivo to the creek (Fig. 4). Potential sources for shell transport mechanisms include elevated water energy; activities of predators, including raccoons and birds (Stempien 2007); and an extensive history of experimental and research activities at the location. Despite this hypothesized transport, in vivo morphological variation among sample sites is generally preserved in death assemblages.

It is notable that such strongly diverging intraspecific patterns in body size and morphotypes related to environmental gradients are produced over such small spatial scales (a few tens of meters). The accumulation of greater variation within death assemblages from that found among ecological snapshots of live-collected specimens results from the superimposition of a time-averaging signal onto environmentally influenced, perhaps ecophenotypic, patterns of size and shape. This accumulation is even more remarkable when one considers the small amount of time over which these death assemblages have been accumulating. Argyle Lagoon is an anthropogenic feature demarcated from the waters of North Bay by the construction of two spits

connected to what was once an island (Little Island). It is even more remarkable that these spatial patterns can be recorded in the incipient fossil record of a dynamic intertidal environment, suggesting similar patterns could be preserved at a comparable spatial scale in the fossil record.

Parasitism, Body Size, and Morphology.—Digenean trematode parasites in the family Gymnophallidae are known to induce the growth of pits with raised rims on the interior of their bivalve hosts (Ruiz and Lindberg 1989; Huntley and De Baets 2015). These parasites are known to affect their hosts in a number of deleterious ways, including inducing dwarfism or gigantism, castration, and increasing susceptibility to predators (Swennen 1969; Lim and Green 1991; Ballabeni 1995; Taskinen 1998; Hechinger et al. 2009). Within a given sample, bivalves with trematode-induced pits tend to be larger than those without (Huntley and Scarponi 2012; Huntley and De Baets 2015; Scarponi et al. 2017), but this is likely due to hosts accumulating parasites through ontogeny rather than a preference of the parasites. Though creek clams are significantly smaller than lagoon clams, there was no significant difference in size between infested and noninfested clams in either the creek or lagoon live-collected samples (Huntley 2007). The median PC 2 score for parasitized individuals was significantly lower in the lagoon and higher in the creek, respectively, versus nonparasitized individuals (Fig. 4). While these differences in morphology are statistically significant, the fact that they differ in opposite ways between environments suggests that the morphological discrepancies between parasitized and nonparasitized individuals are not ecologically significant. We did not examine death assemblages for parasitic traces due to their comparatively poor preservation. In sum, trematode parasites seem to have little influence on the morphology of *L. staminea*; rather, the morphological variation among creek and lagoon individuals is likely due to differences in environmental and ecological factors, such as hydrodynamic and substrate regimes.

Ecophenotypy, Substrate Heterogeneity, Functional Morphology, and Physiological Trade-Offs.—Ecophenotypy refers to the physical characteristics or behaviors of organisms that result from environmental and/or ecological conditions and not from genetic expression. Do the Argyle clams represent a case of ecophenotypic variation? If so, one would expect that creek and lagoon clams would have the same genotype and express different phenotypes due to environmental disparity. An alternative hypothesis, in which there are two genotypes of clams with distinct phenotypes (blade-shaped and barrel-shaped) experiencing differential recruitment success in the creek and lagoon, could explain the morphological variation without ecophenotypy. While genetic data are not available for these specimens, their physical proximity suggests that the populations are not genetically isolated and were sourced through the same spat-fall events. In this case, ecophenotypy is the most parsimonious interpretation.

Ecophenotypic variation can be related to the functional morphology of the organism and physiological trade-offs (e.g., Bottjer 1980). Bivalves have long served as model organisms for studies in skeletal functional morphology owing to easily observable anatomical features that relate to soft tissue anatomy and physiological function (Stanley 1970). The thin-plate spline analyses and the comparison of 3D models (Fig. 5) of four select valves allow us to elucidate the nature of size-free morphological variation along the PC 1 axis. Positive PC 1 values (typical of lagoon bivalves) are characterized by a deep pallial sinus and contraction of the anterior portion of the shell, the latter of which is directly related to landmarks on the adductor muscle scar. Conversely, specimens with negative PC 1 values (typical of creek bivalves) are characterized by a much shallower pallial sinus and anterior expansion of the shell. Pallial sinus length, relative to overall body size, is positively correlated with the size of the bivalve's siphons and its burrowing depth (Stanley 1970). It follows that lagoon bivalves, which are able to freely burrow in fine-grained substrate, have relatively longer siphons than bivalves occupying the rocky substrate of Argyle Creek in a state of forced epifaunality. We interpret the relatively long pallial sinus of lagoon clams to be the typical morphology of

L. staminea and the reduced pallial sinus of creek clams to be an ecophenotypic variant.

Perhaps nonburrowing creek bivalves divert energy from growing unnecessarily large siphons into other anatomical features that help them cope with elevated water energy and an imposed epifaunal life mode. A visual examination of the expansion factors from the thin-plate spline analyses (Fig. 5) could suggest differences in the relative size of posterior and anterior adductor muscle scars by environment. However, there is no significant environmental variation in the allometric coefficient of either the anterior or posterior adductor muscle scars as indicated by nearly identical reduced major axis (RMA) regression slopes (Fig. 6). This observation is further illustrated by no significant difference in median natural log muscle scar area:natural log centroid-size ratios by environment (Fig. 6). Any seeming morphological dissimilarity between creek and lagoon clams in the allometric analysis of muscle scars is the result of significant body-size differences between the two populations (Figs. 3, 6). Indeed, the lagoon clams are larger, on average, than the creek clams. There is, however, a significant difference in the allometric coefficient of the pallial sinus between creek and lagoon populations (Fig. 6) that is not the spurious result of differences in body size, as also similarly illustrated by the significant difference in median natural log sinus length: natural log centroid-size ratios (Fig. 6).

The analyses conducted thus far have been based upon reduced dimensionality of 3D objects projected onto 2D planes. The comparison of 3D models derived from handheld laser scanning (e.g., Motani 2005; Adams et al. 2010; Platt et al. 2010) can provide a more complete view of morphological change between populations. Specifically, a technique commonly used for tolerance analysis in manufacturing, wherein the topographic deviance between the surfaces of two comparable 3D objects is quantified. In addition to illustrating the strong difference in relative pallial sinus length between the two PC 1 exemplar specimens, the surface comparisons reveal that high PC 1 scores (typical of lagoon bivalves, ALs16 vs. AC17; Fig. 5) are associated with an interior surface that is elevated in the center and suppressed along the commissural margin. Conversely, low PC 1 scores (typical of creek bivalves, AC 17 vs. ALs16; Fig. 5) have a topographically lower center interior surface and slightly elevated commissural margin. In other words, the burrowing lagoon clams have a more compressed obesity index (height/width), and epifaunal creek clams tend to be more inflated. The trends in 3D morphology along PC 2 are less straightforward. Stanley (1970) demonstrated that rapid-burrowing bivalves tend to be shaped like disks, blades, or cylinders (i.e., relatively compressed like the burrowing lagoon clams), and slow burrowers tend to have spherical forms, similar to creek clams. We suggest that the lack of opportunity to burrow alone is not enough to induce such ecophenotypic variation. Rather, we hypothesize that the more inflated morphology of creek clams functions to increase shell strength and stability in a high-energy environment on a rocky substrate.

Conclusions

Common suspension-feeding intertidal bivalves from the northern Pacific coast of the United States display strong variation in size and morphology within a few tens of meters of one another. This variation is related to stark divergences in environment and life mode. Live-collected infaunal bivalves in a fine-grained, low-energy lagoon are larger, more compressed, and have relatively larger siphons than their conspecific counterparts that are forced to be epifaunal in a high-energy, rocky tidal creek. The fidelity of ecophenotypy is quite high, and these results demonstrate the potential for being recorded in the fossil record. Generally, a greater variation in size and shape is recorded in the death assemblages relative to the live-collected specimens. The increase in variance of size and shape, the expected result of temporal and spatial averaging, is likely due in this case to the mixing of multiple generations of individuals, shell transport via hydrodynamics and predatory activities, and temporal limitations on sampling the live fauna. We suggest that the ecophenotypic variation documented in this case study is induced by strong differences in water energy and substrate type and results in physiological

trade-offs that divert energy from the growth of an organ associated with feeding, respiration, and burrowing to a morphology that promotes stability and strength.

Acknowledgments

We gratefully acknowledge the constructive comments of T. Olszewski, a second anonymous reviewer, and M. Patzkowsky (editor). This work has been generously supported by the Peck and Sando Scholarship Funds of the Department of Geological Sciences at the University of Missouri (to T.D.A.) and the G. Ellsworth Huggins Scholarship of the University of Missouri (to J.S.B.). J.W.H. is supported by the National Science Foundation EAR CAREER-1650745. J.D.S. is supported by the National Science Foundation EAR CAREER-1652351 and EAR/IF-1636643.

Literature Cited

Adams, T. L., C. Strganac, M. J. Polcyn, and L. L. Jacobs. 2010. High resolution three-dimensional laser-scanning of the type specimen of *Eubrontes* (?) *glenrosensis* Shuler, 1935, from the Comanchean (Lower Cretaceous) of Texas: implications for digital archiving and preservation. Palaeontologia Electronica 13(3). http://palaeo-electronica.org/2010_3/226/index.html, accessed 7 July 2017.

Ballabeni, P. 1995. Parasite-induced gigantism in a snail: a host adaptation? Functional Ecology 9:887–893.

Berta, A. 1976. An investigation of individual growth and possible age relationships in a population of *Protothaca staminea* (Mollusca: Pelecypoda). PaleoBios 21:1–26.

Bottjer, D. J. 1980. Branching morphology of the reef coral *Acropora cervicornis* in different hydraulic regimes. Journal of Paleontology 54:1102–1107.

Bush, A. M., M. G. Powell, W. S. Arnold, T. M. Bert, and G. M. Daley. 2002. Time-averaging, evolution, and morphologic variation. Paleobiology 28:9–25.

Clewing, C., F. Riedel, T. Wilke, and C. Albrecht. 2015. Ecophenotypic plasticity leads to extraordinary gastropod shells found on the "Roof of the World.". Ecology and Evolution 5:2966–2979.

Coan, E. V., and P. Valentich-Scott. 2012. Bivalve seashells of tropical west America. Marine bivalve mollusks from Baja California to northern Peru. Santa Barbara Museum of Natural History, Santa Barbara, Calif.

Collins, K. S., and M. F. Gazley. 2017. Does my posterior look big in this? The effect of photographic distortion on morphometric analyses. Paleobiology 43:508–520.

Daley, G. M. 1999. Environmentally controlled variation in shell size of *Ambonychia* Hall (Mollusca: Bivalvia) in the type Cincinnatian (Upper Ordovician). Palaios 14:520–529.

Hammer, Ø., D. A. T. Harper, and P. D. Ryan. 2001. PAST: paleontological statistics software package for education and data analysis. Palaeontologica Electronica 4. http://palaeo-electronica.org/2001_1/past/issue1_01.htm, accessed 19 March 2015.

Hechinger, R. F., K. D. Lafferty, F. T. Mancini, III, R. R. Warner, and A. M. Kuris. 2009. How large is the hand in the puppet? Ecological and evolutionary factors affecting body mass of 15 trematode parasitic castrators in their snail host. Evolutionary Ecology 23:651–667.

Huber, M. 2010. Compendium of bivalves. ConchBooks, Hackenheim, Germany.

Hughes, W. W., and C. D. Clausen. 1980. Variability in the formation and detection of growth increments in bivalve shells. Paleobiology 6:503–511.

Hunt, G. 2004a. Phenotypic variation in fossil samples: modeling the consequences of time-averaging. Paleobiology 30:426–443.

——. 2004b. Phenotypic variance inflation in fossil samples: an empirical assessment. Paleobiology 30:487–506.

Huntley, J. W. 2007. Towards establishing a modern baseline for paleopathology: trace-producing parasites in a bivalve host. Journal of Shellfish Research 26:253–259.

Huntley, J. W., and K. De Baets. 2015. Trace fossil evidence of trematode–bivalve parasite–host interactions in deep time. Advances in Parasitology 90:201–231.

Huntley, J. W., and D. Scarponi. 2012. Evolutionary and ecological implications of trematode parasitism of modern and fossil northern Adriatic bivalves. Paleobiology 38:40–51.

Kassambara, A. 2017. ggpubr: 'ggplot2' based publication ready plots. R package, Version 0.1.5. https://CRAN.R-project.org/package=ggpubr, accessed 24 September 2017.

Kassambara, A., and F. Mundt. 2017. factoextra: extract and visualize the results of multivariate data analyses. R package, Version 1.0.5. https://CRAN.R-project.org/package=factoextra, accessed 9 October 2017.

Kemp, P., and M. D. Bertness. 1984. Snail shape and growth rates: evidence for plastic shell allometry in *Littorina littorea*. Proceedings of the National Academy of Sciences USA 81:811–813.

Kidwell, S. M., and S. M. Holland. 2002. The quality of the fossil record: implications for evolutionary analyses. Annual Review of Ecology and Systematics 33:561–588.

Kozloff, E. N. 2000. Seashore life of the northern Pacific coast: an illustrated guide to northern California, Oregon, Washington, and British Columbia. University of Washington Press, Seattle, Wash.

Krause, R. A., Jr. 2004. An assessment of morphological fidelity in the sub-fossil record of a terebratulide brachiopod. Palaios 19:460–476.

Lazo, D. G. 2004. Bivalve taphonomy: testing the effect of life habits on the shell condition of the littleneck clam *Protothaca* (*Protothaca*) *staminea* (Mollusca: Bivalvia). Palaios 19:451–459.

Legendre, P. 2014. lmodel2: model II regression. R package, Version 1.7-2. https://CRAN.R-project.org/package=lmodel2, accessed 16 August 2017.

Lim, S. S. L., and R. H. Green. 1991. The relationship between parasite load, crawling behaviour, and growth rate of *Macoma balthica* (L.) (Mollusca, Pelecypoda) from Hudson Bay, Canada. Canadian Journal of Zoology 69:2202–2208.

Motani, R. 2005. Detailed tooth morphology in a durophagous ichthyosaur captured by 3D laser scanner. Journal of Vertebrate Paleontology 25:462–465.

Penny, A. M., R. A. Wood, A. Yu. Zhuravlev, A. Curtis, and F. Bowyer. 2017. Intraspecific variation in an Ediacaran skeletal metazoan: *Namacalathus* from the Nama Group, Namibia. Geobiology 15:81–93.

Piovesan, E. K., C. T. Bergue, G. Fauth, and M. C. Viviers. 2015. Palaeoecology of ostracods from the Late Cretaceous from northeastern Brazil and its relation to sequence stratigraphy. Palaeogeography, Palaeoclimatology, Palaeoecology 424:40–48.

Platt, B. F., S. T. Hasiotis, and D. R. Hirmas. 2010. Use of low-cost multistripe laser triangulation (MLT) scanning technology for three-dimensional, quantitative paleoichnological and neoichnological studies. Journal of Sedimentary Research 80:590–610.

R Core Team. 2017. R: a language and environment for statistical computing. R Foundation for Statistical Computing, Vienna, Austria. https://www.R-project.org.

Ruiz, G. M., and D. R. Lindberg. 1989. A fossil record for trematodes: extent and potential uses. Lethaia 22:431–438.

Scarponi, D., M. Azzarone, M. Kowalewski, and J. W. Huntley. 2017. Surges in trematode prevalence linked to centennial-scale flooding events in the Adriatic. Scientific Reports ar5732. doi: 10.1038/s41598-017-05979-6.

Schlüter, N. 2016. Ecophenotypic variation and developmental instability in the Late Cretaceous echinoid *Micraster brevis* (Irregularia; Spatangoida). PLoS ONE 11:e0148341. doi: 10.1371/journal.pone.0148341.

Schneider, C. A., W. S. Rasband, and K. W. Eliceiri. 2012. NIH Image to ImageJ: 25 years of image analysis. Nature Methods 9:671–675.

Stanley, S. M. 1970. Relation of shell form to life habits of the bivalvia (Mollusca). Geological Society of America Memoir 125.

Stempien, J. A. 2007. Detecting avian predation on bivalve assemblages using indirect methods. Journal of Shellfish Research 26:271–280.

Swennen, C. 1969. Crawling-tracks of trematode infected *Macoma balthica* (L.). Netherlands. Journal of Sea Research 4:376–379.

Taskinen, J. 1998. Influence of trematode parasitism on the growth of a bivalve host in the field. International Journal of Parasitology 28:599–602.

Wickham, H. 2009. ggplot2: elegant graphics for data analysis. Springer, New York.

——. 2011. The split-apply-combine strategy for data analysis. Journal of Statistical Software 40:1–29.

Wickham, H., R. Francois, L. Henry, and K. Müller. 2017. dplyr: a grammar of data manipulation. R package, Version 0.7.2. https://CRAN.R-project.org/package=dplyr, accessed 20 August 2017.

Wilk, J., and R. Bieler. 2009. Ecophenotypic variation in the Flat Tree Oyster, *Isognomon alatus* (Bivalvia: Isognomonidae), across a tidal microhabitat gradient. Marine Biology Research 5:155–163.

Wilke, C. O. 2017. ggridges: ridgeline plots in 'ggplot2'. R package, Version 0.4.1. https://CRAN.R-project.org/package=ggridges, accessed 20 August 2017.

Wilson, M. V. H. 1988. Taphonomic processes: information loss and information gain. Geoscience Canada 15:131–148.

Zieritz, A., and D. C. Aldridge. 2009. Identification of ecophenotypic trends within three European freshwater mussel species (Bivalvia: Unionoida) using traditional and modern morphometric techniques. Biological Journal of the Linnean Society 98:814–825.